Philosophical Transactions Of The Royal Society A-mathematical Physical And Engineering Sciences
January 2023, Volume 381 Issue 2240 Pages 20210221 (14p.)
https://doi.org/10.1098/rsta.2021.0221
https://archimer.ifremer.fr/doc/00806/91826/

Characterization and modelling of the hygro-viscoelastic behaviour of polymer-based composites used in marine environment

Dezulier Quentin [1], Clement Alexandre [1,*], Davies Peter [2], Jacquemin Frédéric [1], Arhant Mael [2], Flageul Benjamin [2]

[1] Nantes Université, CNRS, GeM, UMR 6183, 44600 Saint-Nazaire, France
[2] IFREMER ,Centre Bretagne, Marine Structures Laboratory, 29280 Plouzané, France

* Corresponding author : Alexandre Clement, email address : alexandre.clement@univ-nantes.fr

Abstract :

This paper presents results from a study of the long-term behaviour of carbon/epoxy composites. The interactions between ageing in water and constant mechanical loads are described, first experimentally then using a simple modelling approach. An identification procedure for the model is carried out and test/model comparisons are discussed. The results show that a four-parameter Burgers model can provide a good fit of the experimental data. The analysis of the results indicates the impact of water diffusion on the viscoelastic behaviour with larger strains for both creep and recovery phases. Those changes tend to appear at the early stage of the moisture diffusion process and stabilize quite quickly. This article is part of the theme issue 'Ageing and durability of composite materials'.

Keywords : ageing, creep, viscoelasticity, composite

1. Introduction

The use of continuous fiber reinforced composites is now widespread, particularly in the marine industry, and several references describe their use in structures from small boats to military ships and submarines [1-4]. More recent applications include marine energy recovery systems such as the blades of tidal turbines; these impose more complex constraints, as they are destined to be permanently installed in high energy environments where inspection and maintenance are difficult and costly. There is thus a need to guarantee long term reliability, and

validated models of long term behaviour are essential. The durability of composite materials is a complex subject, grouping the effects of environmental aging, creep, and cyclic loading [5,6]. While these effects have been considered independently in numerous studies, a more realistic representation of behaviour under marine service conditions must include the coupling between them. This is one of the aims of the present work. However, first some examples of previous studies will be given, in order to highlight the current state of the art in this field.

The influence of water on continuous fibre reinforced thermosetting polymers has been studied in some detail in the past. Weitsman provided an excellent overview of published work [7], while Colin & Verdu [8] gave a detailed description of the role of the matrix. In general, water, whether distilled or seawater, will diffuse into the matrix resulting in reversible swelling and plasticization mechanisms. Various kinetic models have been proposed for diffusion [9], but in many cases the 1-D Fickian diffusion model proposed by Springer and colleagues over 40 years ago provides a reasonable first estimate of the water profile [10]. Then at longer times the matrix may hydrolyze, a chemical ageing mechanism resulting in permanent molecular chain scission. This can result in matrix cracking, which in turn encourages additional diffusion and accelerating degradation. In parallel, ageing may also degrade the fibre/matrix interphase region; this may occur more quickly than matrix degradation if the interphase facilitates water entry [11]. One of the difficulties in predicting long term behaviour of composites is that, even without considering mechanical loading, these four mechanisms (plasticization, swelling, hydrolysis and interface degradation) can occur simultaneously, each with its own kinetics. Another factor to consider is the temperature. Raising the water temperature is often used in laboratory studies to accelerate water ingress but temperature variations in service will also affect the quantity of water in the material.

There are then various coupling effects between these mechanisms to be considered. The first involves the influence of absorbed water on short term composite mechanical behaviour, and this is the easiest to study. Samples can be immersed in water and removed periodically for testing. Many examples of this type of study are available such as [12-15]. A second aspect, requiring additional test equipment, involves measuring how mechanical loads affect the water take-up. Early work by Fahmi & Hurt on epoxy polymers [16] was followed by several studies showing that applied stress can increase water uptake [17-19]. So, given that water affects mechanical properties and that mechanical loading affects water absorption it is easy to imagine that strong coupling between the two will seriously affect long term behaviour. An additional factor to include in the durability analysis is the time-dependent behaviour of polymer composites, and there have been many studies of the response of composites to constant loads, or creep. For example, Scott et al. provided a review of studies

pre-1995 [20]. Work at Virginia Polytechnic in the 1980's [21,22] resulted in the development of viscoelastic models, including the non-linear viscoelastic approach of Schapery [23].

Results showing how moisture affects creep behaviour are less frequent, but those which exist have indicated that water ingress can accelerate creep strain [24-29]. Time-temperature superposition has been used by a number of authors to produce master curves, with Miyano and Nakada in particular applying this approach successfully to predict a range of composite properties [30]. An equivalence between temperature and water content with respect to creep behaviour has also been described [31]. Finally, Raghavan and colleagues have studied damage development under creep loading [32, 33], while other studies have used load-unload and isostress cycles to identify creep and recovery parameters [34, 35]. A large number of creep models have been applied to composites; Guedes provided a review of life prediction methods [36], and the different models will be discussed in more detail below.

The aim of the present paper is to highlight the various mechanisms leading to changes in mechanical properties of composites immersed in water for long periods, so that their effects can be included in structural design. We focus in particular on water diffusion impact on extended mechanical loadings: we thus proposed specific creep-recovery test sequences for unaged and aged composite samples. After analysis of the results from those latter tests, we use a viscoelastic modelling approach, based on a Burgers model [37, 39] which has been used for instance in [40-43] for different composite materials. We analyze the effect of water diffusion on identified parameters and show that the proposed model is also predictive regarding other external loadings.

The paper is organized as follows. Section 2 deals with the studied composite material. We first describe the manufacturing process of the samples used for hygroscopic and mechanical tests. We then propose a model of the water diffusion process associated with the identifications of its parameters showing that a dual-stage Fick model is a good candidate here. Hygroscopic expansion measurements and mechanical tensile tests end this section to highlight the impact of water absorption on the mechanical behaviour. Section 3 present the long-term behaviour of the composite material with comparisons between unaged and aged samples with creep-recovery test sequences. We then propose a model of the viscoelastic behaviour based on a four element Burgers model. The results of the identification for the different creep phases and the various ageing cases are analyzed in order to highlight the effect of water diffusion on the latter behaviour. Some concluding remarks and perspectives are finally drawn in Section 4.

2. Materials & hygro-viscoelastic characterization

2.1.Materials

The material investigated in this study is a high-performance carbon/epoxy laminate produced in an autoclave by FMC composites (Brest). Composite panels $[\pm 45]_6$ were obtained by stacking 6 composite plies with an areal weight of 350 g/m², where each ply was produced from the winding of towpregs around a mandrel. These towpregs were supplied by Vitech Composites and are impregnated with an epoxy resin from Huntsman (LY556). Panels were then cured in an autoclave at 120°C for 2 hours with a pressure of 6 bars. Mean final thickness of the panels was 2.02 mm. Fibre volume fraction and glass transition temperature were measured to be 58.1 ± 0.8 % and 108°C (onset value) respectively. Finally, specimens for weight gain measurements (50 x 50 x 2 mm³), hygroscopic expansion (200 x 20 x 2 mm³) and tensile and creep tests (250 x 25 x 2 mm³) were obtained by water jet cutting.

2.2.Ageing

2.2.1. Water diffusion

Weight measurements were performed in deionized water, at 25°C to follow the weight gain during water immersion and also at 60°C to accelerate water diffusion. Weight gain was followed through periodic weighing of the different specimens on a Sartorius LA310S balance with a precision of 0.1 mg. The weight gain $C(t)$ was calculated from Equation (1):

$$C(t) = \frac{m(t) - m_0}{m_0} \quad (1)$$

where $C(t)$ is the mass of the sample at a given time t and m_0 is the initial dry mass. For each ageing condition, 3 samples were weighed over 18 months.

2.2.2. Identification of the water diffusion behavior

Based on the experimental data obtained through weight measurements, it is possible to examine the water diffusion kinetics through the identification of the water diffusion behavior. In the literature, the most common way to describe the water diffusion behavior in polymers and composites is Fick's model [10], shown in Equation (2), where two parameters can be determined: the diffusion coefficient D and the water concentration at saturation C_{sat}.

$$C(t) = C_{\text{sat}}\left(1 - \frac{8}{\pi^2}\sum_{n=0}^{\infty}\frac{1}{(2n+1)^2}exp\left[-(2n+1)^2\pi^2.\frac{D.t}{e^2}\right]\right) \quad (2)$$

However, while Fick's model is often used to describe water diffusion kinetics in polymers and composites, it does not always describe the water ingress accurately [9]. Figure 1-Left illustrates the experimental sorption kinetics for the composite at the two studied temperatures: we can observe anomalies of diffusion implying that the application of Fick's model will not be accurate. We can clearly observe a second stage of diffusion and it is apparent that the saturation state has not been reached for any of the temperature conditions.

Alternatives, such as the dual-stage Fick model can be more appropriate when two distinct water diffusion mechanisms are identified, Equation (3).

$$C(t) = \sum_{i=1}^{2}\left[C_{\text{si}}\left(1 - \frac{8}{\pi^2}\sum_{n=0}^{\infty}\frac{1}{(2n+1)^2}exp\left[-(2n+1)^2\pi^2.\frac{D_{\text{i}}.t}{e^2}\right]\right)\right] \quad (3)$$

In this case two different diffusion coefficients, D_1 and D_2, can be identified, together with two different water concentrations C_{s1} and C_{s2}. Identification is then based on a least squares minimization solution. The results of the identification procedure are shown on Figure 1-Right where there is a very good agreement between the experimental data and the identified sorption curves. Table 1 provides the identified dual-stage Fick parameters for each temperature condition.

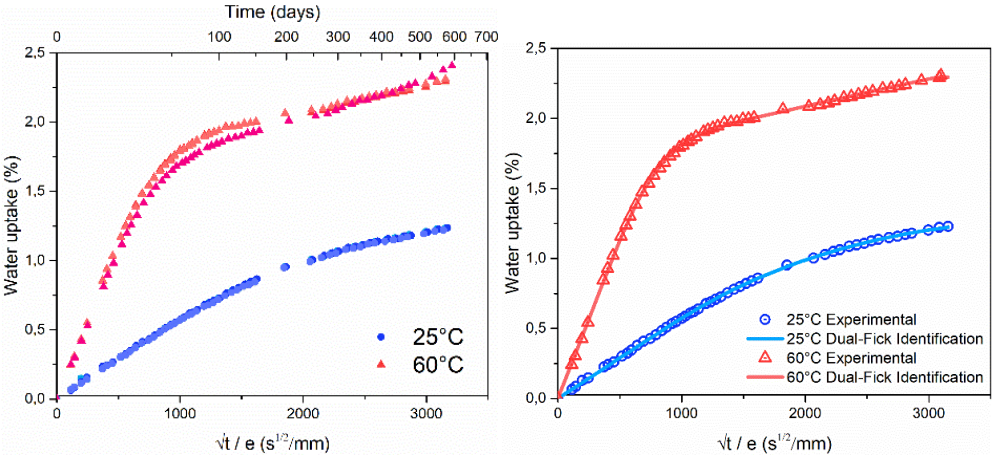

Figure 1: Gravimetric measurements performed on composite samples at 25°C and 60°C water: raw data (left) and identified Fick curves with mean data points (right).

One should note that the second water concentration denoted by C_{s2} may not be the "true" physical value since the saturated state has not been reached and that this state may never be reached, depending on the very long-term behaviour of the diffusion process. Moreover, the identified values for each parameter are very different:

for instance, at 25°C, the ratio $\frac{D_1}{D_2}$ is close to 3.5 whereas the value at 60°C is close to 50. This latter remark underlines the strong influence of temperature on the hygroscopic behaviour of the studied composite material.

Dual-stage Fick parameters	**25°C**	**60°C**
C_{s1} (%)	0.39 ± 0.07	1.25 ± 0.31
D_1 (m²/s)	(9.34 ± 0.93). 10^{-14}	(2.76 ± 0.16). 10^{-13}
C_{s2} (%)	0.92 ± 0.04	1.69 ± 0.02
D_2 (m²/s)	(2.14 ± 0.24). 10^{-14}	(5.67 ± 4.01). 10^{-15}

Table 1: Identified dual-stage Fick parameters for each studied temperature.

2.2.3. Hygroscopic expansion

Hygroscopic swelling is directly associated with water absorption. In order to measure this, periodic measurements were carried out using a Keyence LK-G32 laser with a precision of about 5 µm. The induced hygroscopic strain ε_h is determined using Equation 4.

$$\varepsilon_h = \frac{L(t) - L_0}{L_0} \times 100 \qquad (4)$$

where L(t) is the length of the tested specimen at an ageing time t and L_0 the initial length of the specimen.

Figure 2 shows the experimental hygroscopic expansion ε_h measured in the longitudinal and transverse (through-thickness) directions for both temperature conditions. The results are similar for both temperatures. Moreover, this expansion is only significant for the transverse (*i.e.* thickness) direction and can be neglected in the longitudinal direction.

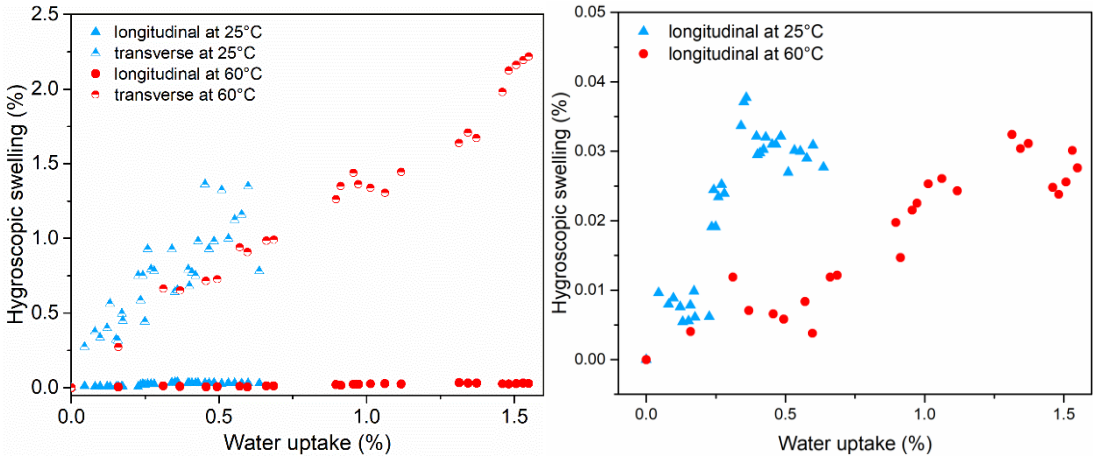

Figure 2: Hygroscopic swelling in longitudinal and thickness directions of ±45° laminates (left) and zoom for the transverse direction (right) for both temperature conditions.

2.3.Mechanical characterization

Two different types of mechanical test were performed within this study, tensile quasi-static tests and tensile creep. These were performed at four different stages: in the unaged state (named T_0) and then for three different ageing conditions in immersion at 25°C and denoted by T_1 = 55 days, T_2 = 392 days and T_3 =527 days: those times respectively correspond to global water contents of 0.6%, 1.2% and 1.3%. It may be noted that ageing was here only carried out at 25°C. For each condition, three repeat specimens were characterized.

2.3.1. Quasi static tests

Quasi-static tensile tests were performed according to ISO 527 on a Roell & Korthaus™ testing machine using a 200 kN load cell at a crosshead speed of 2 mm/min. During these tests, strain was recorded by Digital Image Correlation (DIC) using a Basler camera (aca2500 20gm) and the Aramis™ software from GOM.

Figure 3 illustrates the results of those tensile tests for unaged and aged composite specimens. First, we note that sample failures occur at high strain levels around 15% whatever the ageing time. Nevertheless, water diffusion within the material lowers the stress levels at for equivalent strains. Moreover, the higher the time of ageing or global water content, the lower the stresses.

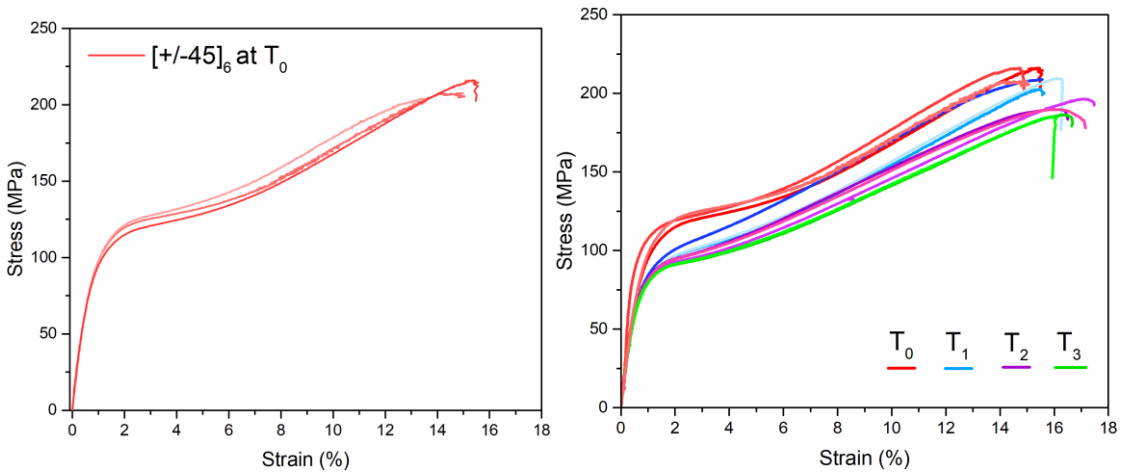

Figure 3: Results of tensile tests at T_0 (left) and comparisons with various times of ageing at T = 25°C (right).

2.3.2. Creep-recovery tests

Creep tests were performed on an Instron™ testing machine (5566) following a specific test sequence where seven incremental creep levels were investigated. Each level combines an initial creep step of 1 hour followed

by a recovery of 3 hours, so each test sequence lasts 28 hours. Creep levels were defined based on the elastic limit σ_e determined from quasi static tests in the unaged state and ranged from 25% up to 125% of σ_e, see Table 2. Using such a sequence provides a characterization of both the viscoelastic behaviour ($\sigma<\sigma_e$) and the nonlinear viscoplastic behaviour ($\sigma>\sigma_e$).

Creep step	1	2	3	4	5	6	7
% of σ_e	25	50	75	100	110	120	125
σ [MPa]	22.75	45.5	68.25	91	100.1	109.2	113.75
F [N]	1138	2275	3412	4550	5005	5460	5688

Table 2: Elastic limit σ_e, applied stresses σ and imposed forces F for each step of creep tests.

Figure 4 shows the results of those tests for unaged specimens and Figure 5 illustrates the same tests for each ageing time, allowing an analysis of the impact of water diffusion. On Figure 4, we can observe very high residual strains especially from step 4 corresponding to 91 MPa and 100% of the initial elastic limit. Moreover, from step 5, *i.e.* for applied stresses superior to the elastic limit, we notice a significant variability which may come from the accumulation of residual strain and the activation of damage mechanisms such as crack propagation or debonding.

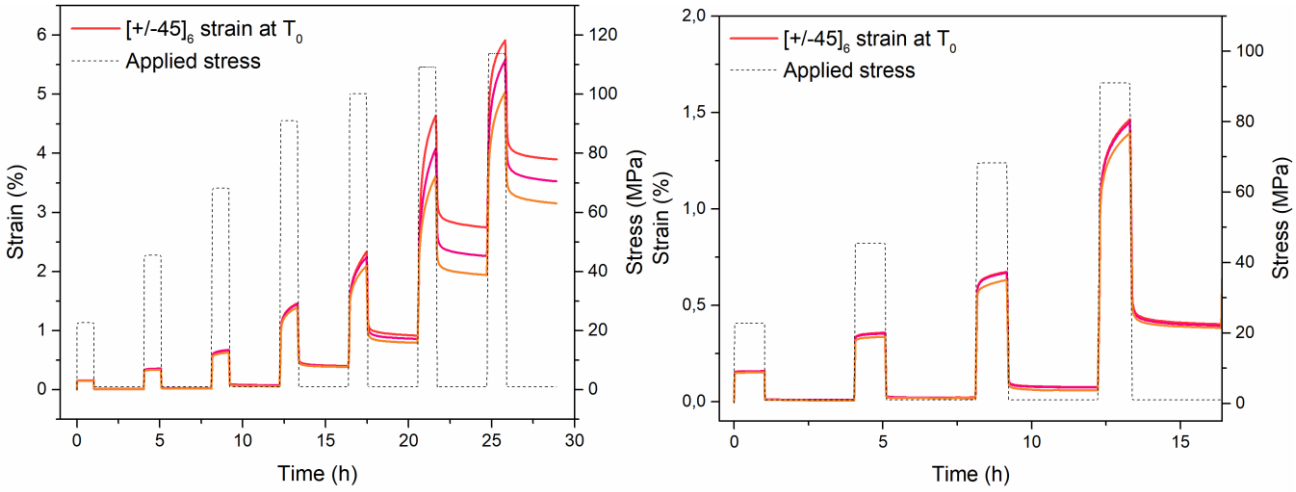

Figure 4: Creep-recovery tests at T_0 for the 7 step creep-recovery sequence (left) and focus on the first four steps (right).

On figure 5, where the creep-recovery tests for aged conditions are shown, we clearly observe the impact of water diffusion from step 3 *i.e.* an applied stress of 68.25 MPa. First, we note higher viscoelastic strains for the

aged samples with a similar behaviour for ageing times T_2 and T_3 since they correspond to similar water contents of 1.2% and 1.3%. Second, we see that residual strain greatly increases with respect to the unaged case T_0. Finally, one should note that tests at times T_2 and T_3 had to be stopped since the viscoelastic strains became too large.

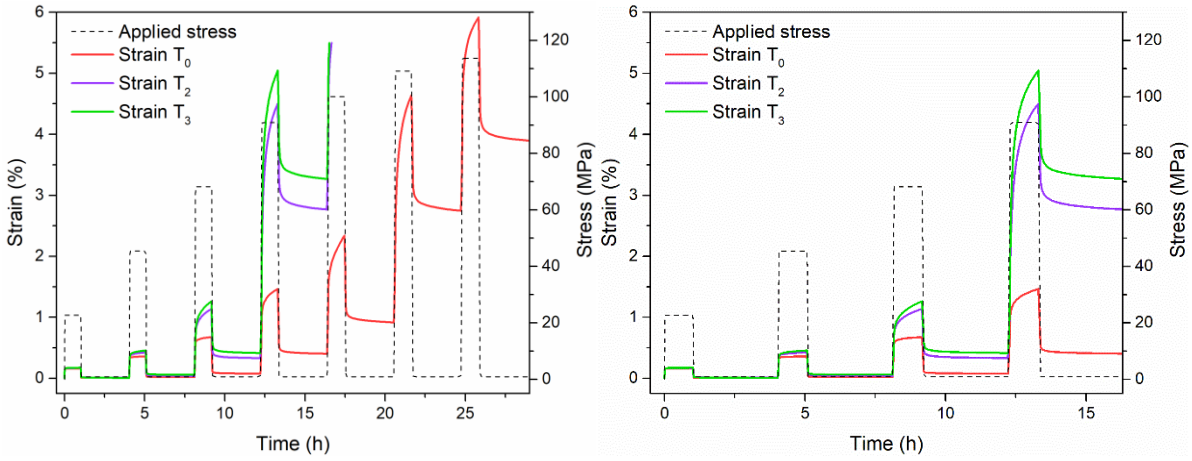

Figure 5: Creep-recovery tests for unaged and aged samples for the 7 steps creep-recovery sequence (left) and focus on the first four steps (right).

3. Viscoelastic modelling and results

This section is devoted to the modelling of the viscoelastic behaviour of the studied composites and the associated analyses.

3.1.Rheological model

Strain curves depicted on Figures 3 and 4 show the total strain ε defined by

$$\boldsymbol{\varepsilon = \varepsilon_0 + \varepsilon_{ve} + \varepsilon_h} \tag{5}$$

where ε_0 is the instantaneous strain corresponding to the purely elastic behaviour, ε_{ve} is the viscoelastic strain and ε_h is the hygroscopic strain related to the water content. However, since the hygroscopic strain is very low in the longitudinal direction as shown on Figure 2, it can be neglected and then $\varepsilon_{tot} \cong \varepsilon_e + \varepsilon_{ve}$.

Figures 4 and 5 show a viscoelastic behaviour with nonlinearities and simple models such as Maxwell or Kelvin-Voigt are then not suitable. We thus propose to use a four element Burgers model [37, 39] which can represent this type of viscoelastic behaviour more accurately. This model results from a combination of a Kelvin-Voigt model and a Maxwell model in series.

The constitutive equation describing the Burgers model was suggested by Findley et al. [39] and can be written as follows:

$$\sigma + \left(\frac{\eta_1}{E_1} + \frac{\eta_1}{E_2} + \frac{\eta_2}{E_2}\right)\dot{\sigma} + \frac{\eta_1\eta_2}{E_1E_2} = \eta_1\dot{\varepsilon} + \frac{\eta_1\eta_2}{E_2}\ \ddot{\varepsilon} \tag{6}$$

where E_1 and E_2 are two stiffness related parameters and η_1 and η_2 two damping related parameters. Considering creep strain, this equation can then be expressed using a Laplace transformation as shown in Equation (7):

$$\varepsilon\,(t) = \frac{\sigma_0}{E_1} + \frac{\sigma_0}{E_2}(1 - \exp(\frac{-E_2.t}{\eta_2})) + \frac{\sigma_0}{\eta_1}t \tag{7}$$

where σ_0 is the applied stress. Therefore, four parameters need to be identified: E_1, E_2, η_1 and η_2. Elastic modulus E_1 can be found easily, knowing the applied stress σ_0 and the instantaneous strain ε_0 such that $E_1 = \sigma_0 / \varepsilon_0$. The identification of the other three parameters is not straightforward and an optimization problem is proposed to circumvent this issue. The aim is to find the optimal parameters $(\underline{E_2}, \underline{\eta_1}, \underline{\eta_2})$ by minimizing the least-square discrepancy q between the N experimental data points $\{\varepsilon_{exp}(t_n)\}_{n=1}^{N}$ and the strains $\{\varepsilon_{burger}(t_n)\}_{n=1}^{N}$ obtained with Equation (8) such that:

$$q(E_2, \eta_1, \eta_2) = \sum_{n=1}^{N} (\varepsilon_{burger}(t_n) - \varepsilon_{exp}(t_n))^2 \tag{8}$$

An optimal set $(\underline{E_2}, \underline{\eta_1}, \underline{\eta_2})$ is thus a solution of the following minimization problem:

$$P_{Burger} \ : \ \left(\underline{E_2}, \underline{\eta_1}, \underline{\eta_2}\right) = \quad argmin \quad q(E_2, \eta_1, \eta_2) \tag{9}$$

$$(E_2, \eta_1, \eta_2) \in (\mathbb{R}^+)^3$$

In practice, this optimization problem (9) is solved with a Nelder-Mead simplex algorithm [44] using a random starting point. If no information is available on the parameters to identify, a first coarse localization of a minimum based on several random starting points may help to converge through the optimal solution.

3.2.Results and discussion

We first focus on some identification results. We only applied the model to creep steps 2, 3 and 4 corresponding respectively to applied stresses of magnitude 45.5 MPa, 68.25 MPa and 91 MPa. Experimental results associated to higher applied stresses clearly involve nonlinear phenomena, which cannot be represented with the proposed model. Moreover, we only work on the creep phases here; the recovery phases will be studied in future work. Finally, for the sake of clarity, we only show the viscoelastic strains ε_{ve} as this is easier to interpret than also showing the instantaneous strains ε_e on the same plots. Figure 6 presents the results of the identification for applied stresses of 45.5 MPa and 68.25 MPa, respectively corresponding to 50% and 75% of the estimated initial

elastic limit, and for unaged samples (T_0) and aged samples at times T_2=392 days and T_3= 527 days. One should note that slight differences appear for applied stresses of 68.25 MPa between Figure 5–right and Figure 6-right: the larger gap between the results at T_2 and T_3 comes from the instantaneous elastic strain ε_e which differs for those two times of ageing and which is not shown on Figure 6.

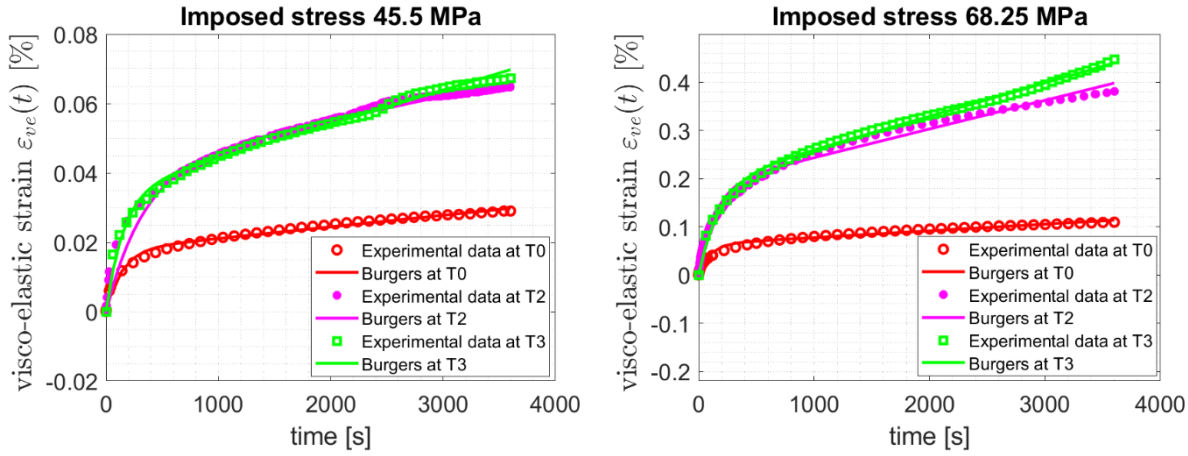

Figure 6: Comparison between experimental data and identified viscoelastic strain obtained with the Burgers model for applied stresses 45.5 MPa (left) and 68.25 MPa (right) for different ageing times.

On Figure 6, we can first observe a very good fit between the experimental observations and the identified curves based on the proposed Burgers model. Then, we also clearly note the effect of water on the viscoelastic behaviour, since curves at time T_0 present lower strains. However, it is interesting to note that the strains for aged times T_2 and T_3 are very close, which indicates that changes in the viscoelastic behaviour appear early during the diffusion process. One should note that this statement is not necessarily true for higher applied stresses as we can see on figure 5. However, in that case the difference between ageing times T_2 and T_3 may be caused by other phenomena such as damage mechanisms, which may be activated by both water diffusion and high applied stresses.

We now propose an analysis of the Burgers parameters E_2, η_1 and η_2 with respect to the applied stresses. This is only performed for times T_0 and T_3 since results for time T_2 are very close to those for T_3. The results are presented on Figures 7, 8 and 9 respectively for η_1, E_2 and η_2. For each case, three samples have been tested and the presented means come from those three samples. We first focus on viscosity η_1, illustrated on Figure 7, which controls the linear evolution of viscoelastic strain during the so-called secondary-creep stage. First, we note a good repeatability of the tests resulting in a low variability for this parameter. Second, we note that viscosity η_1

decreases with respect to the applied stress whatever the ageing time: this indicates that the viscoelastic strain increases faster according to the external loading. Third, we show that this decrease is clearly linear with the applied stress. Moreover, the slopes of each linear approximation shown on Figure 6 for times T_0 and T_3 are very close (differing by about 7%) but the intercepts are different with a lower one for the aged samples. It is thus interesting to note that water diffusion decreases the viscosity η_1 but does not modify its linear behaviour with respect to the applied stress.

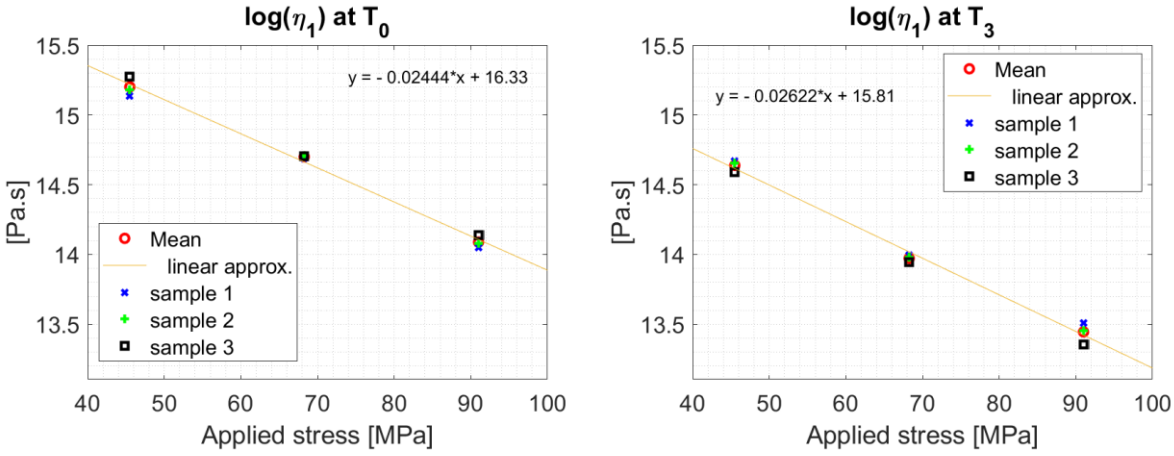

Figure 7: Variations of Burgers parameter η_1 with respect to applied stress for times T_0 (left) and T_3 (right).

We then focus on parameters E_2 and η_2 which govern the transient nonlinear evolution of the viscoelastic strain before the secondary-creep stage. We first analyze the results for apparent modulus E_2 illustrated on Figure 8. As for viscosity η_1, we note lower values for ageing time T_3 and a linear decrease for both times. However, the relative difference between the two slopes, around 32%, is higher but the intercepts are exactly the same. Moreover, the variability on E_2 is higher for ageing time T_3.

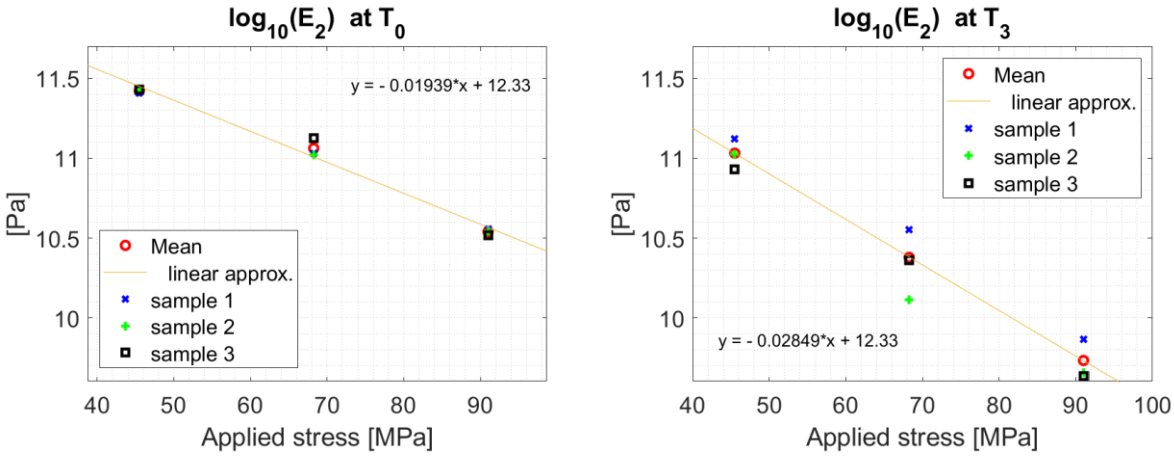

Figure 8: Variations of parameter E_2 with respect to applied stress for times T_0 (left) and T_3 (right).

We finally focus on parameter η_2 for which the results are plotted on Figure 9. As for the previous parameters, a linear approximation gives a good representation of the decrease of the viscoelastic strain with respect to the applied load: we observe a relative difference of 20% between the slopes and very similar values of intercept, as seen for parameter E_2. Once again, the variability on η_2 is higher for ageing time T_3 than for unaged time T_0. To conclude, it is clear that parameters E_2 and η_2 behave in a similar way with respect to to the applied stress, which seems logical since they are both related to the nonlinear part of the viscoelastic evolution with time.

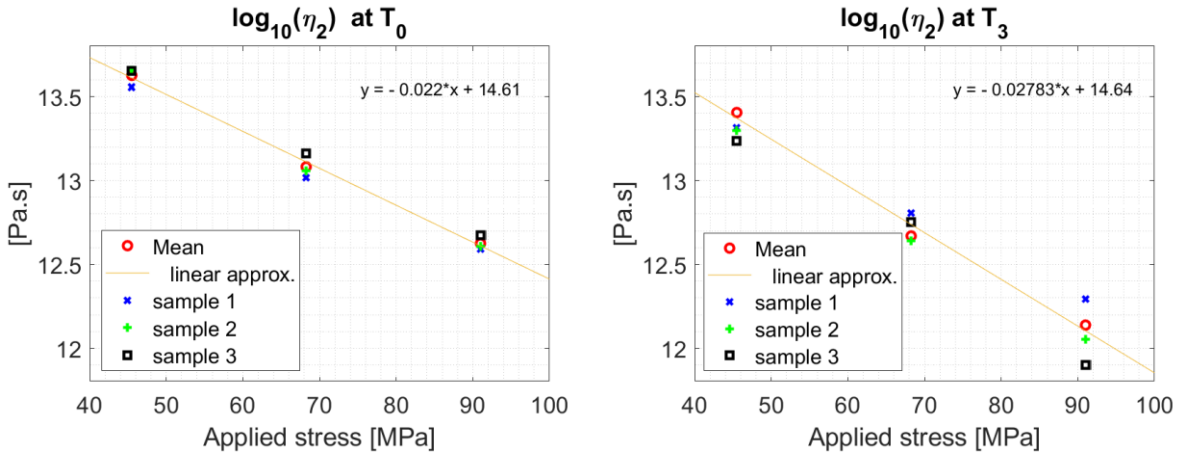

Figure 9: Variations of Burgers parameter η_2 with respect to applied stress for times T_0 (left) and T_3 (right).

We will now show that the previous results with the associated statements may help to predict the viscoelastic behaviour for different times of ageing and applied stresses. To achieve this task, other tests have been conducted for a different ageing time equal to 55 days, denoted T_1 in the following, and for various applied stresses equals to 39 MPa and 59.25 MPa.

Since we have observed that the viscoelastic responses are very close for ageing times T_2 and T_3, we propose to use the previous results for time T_3 to compute the Burgers parameters for time T_1. Those parameters are thus computed from the equations of the linear approximations given on Figures 7, 8 and 9. Comparisons between experimental data and the predicted viscoelastic strains are depicted on Figure 10. The presented results are promising with a very good agreement between the predicted strain curves and the experimental observations for both applied stresses. This also indicates that the Burgers parameters identified for ageing time T_3 can be used for a lower ageing time, *i.e.* T_1 which is equal to 55 days and corresponding to a global water content of 0.6 % that is less than half of the value at T_3. Once again this statement implies that the changes in the viscoelastic behaviour appear early in the diffusion process.

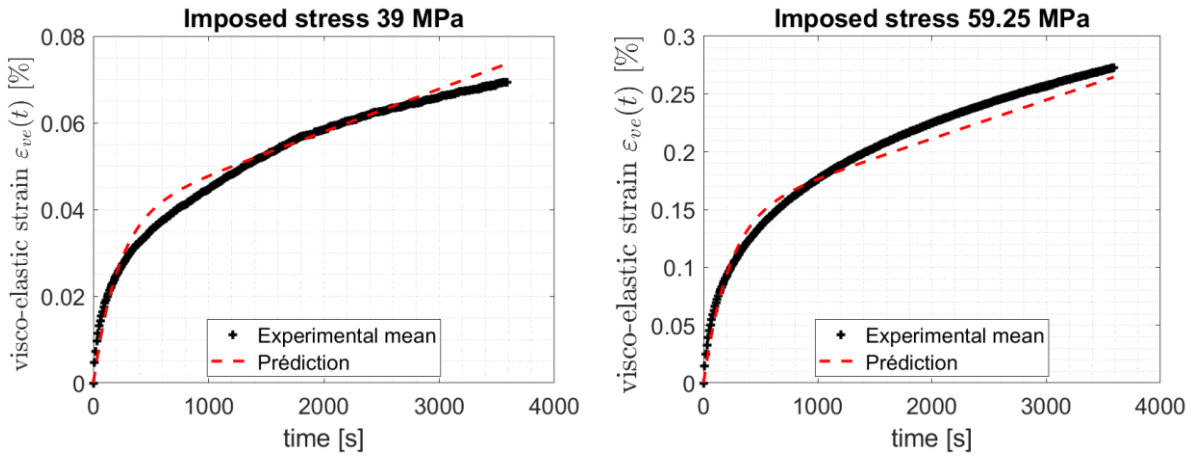

Figure 10: Comparison between experimental data and predictions based on interpolated Burgers parameters for new applied stress 39 MPa (left) and 59.25 MPa (right) at ageing time T_1.

Finally, we illustrate the evolution of the Burgers parameters with ageing time on Figure 11.

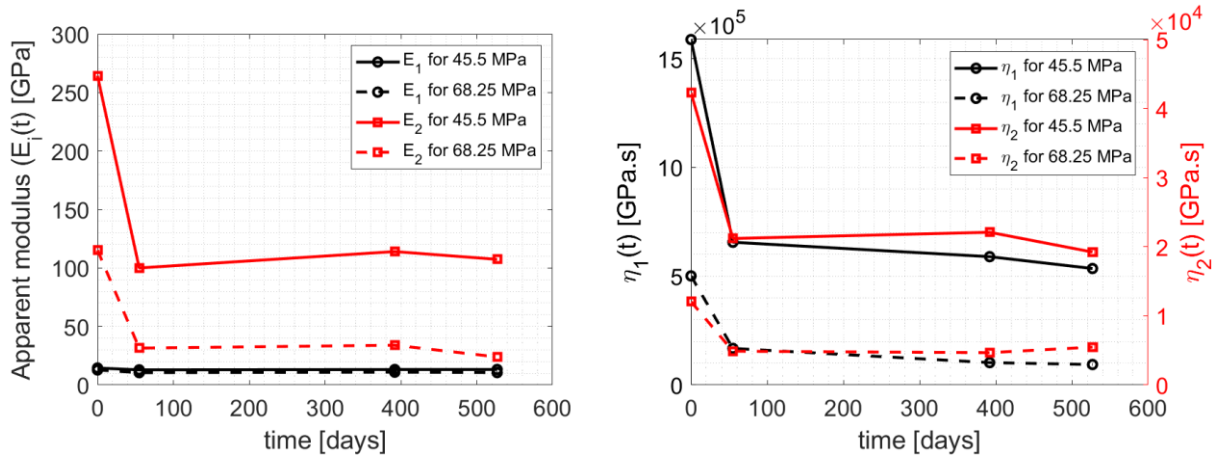

Figure 11: Evolution of identified Burgers parameters with respect to time of ageing: apparent moduli E_1 and E_2 (left) and viscosity η_1 and η_2 (right).

On this latter figure, the values of the parameters for time $T_1 = 55$ days have been determined using the previous strategy for the predicted strain curves. In practice, we compute the values for applied stresses 45.5 MPa and 68.25 MPa from linear interpolation of the applied stresses used for testing at T_1 corresponding to 39.5 MPa, 59.25 MPa and 79 MPa. Figure 11-left shows the results for parameters E_1 and E_2: as expected, apparent elastic modulus E_1 remains the same regardless of applied loads. We only note a slightly lower value for the aged case. The behaviour of parameter E_2 differs greatly from E_1: first, we can note that a significant drop appears at the beginning of ageing for both applied stresses: once again, this indicates that the changes in the viscoelastic

behaviour occur during the very first steps of the water diffusion process. Secondly, parameter E_2 tends to stabilize. Moreover, as seen on Figure 8, one can notice that the E_2 values are lower for the highest applied stress. Figure 11-right presents the same type of analysis for Burgers parameters η_1 and η_2: the same conclusions can be drawn since we can clearly observe that η_1 and η_2 depend on the times of ageing and the applied stresses with a significant drop at the beginning of the diffusion process. However, since no experimental data are available prior to time T_1, no extrapolation of the Burgers parameters can be made with the proposed model for lower times than days. Further tests will be conducted with a finer time-discretization at the very early stage of the diffusion process in order to better analyse the latter behaviour. Changes to the model, if needed, will then be applied.

4. Conclusions

The present work focused on the durability of an epoxy-based composite material. The water diffusion kinetics were experimentally characterized and a dual-stage Fick modelling was used to capture the so-called anomalies of diffusion. We showed that the longitudinal hygroscopic expansion was very low and can be neglected during the mechanical tests. However, tensile tests have exhibited the impact of water on the stresses for a particular strain with lower levels than those obtained for the unaged case. We then have proposed a study of the viscoelastic behaviour when ageing occurs. We highlighted the strong effect of water diffusion on the creep and recovery phases with both showing higher viscoelastic strains. We then proposed a model of the creep phase with a four element Burgers model with an associated identification procedure of its parameters. The analyses of these parameters with respect to both applied stresses and ageing exhibited a linear behaviour of the evolution of each parameter with similar slopes and intersects. Moreover, we showed that the values of those parameters decreased with the time of ageing and tended to quickly stabilize indicating that changes in the viscoelastic behaviour happened in the early stage of diffusion.

Further work will first be devoted to the recovery phase modelling; irreversible strains are observed for significant applied stresses and thus there is a need for nonlinear modelling. Moreover, a numerical implementation of the proposed model in a finite element software will be performed in order to obtain additional information, such as internal stress effects, on various local fields. Second, the validity of the model

will be checked based on long-term creep tests (several months). It is of particular interest to investigate the duration of short-term identification tests required for reliable long-term prediction.

Acknowledgements

This work was performed within the framework of the WEAMEC, West Atlantic Marine Energy Community, and with funding from the CARENE. The authors are also grateful to ONR (Office of Naval Research) through the Solid Mechanics Program, and thank Dr Yapa Rajapakse for his support throughout this project.

References

1. Smith CS, Design of marine structures in composite materials, 1990, Elsevier Applied Science,London.
2. Mouritz AP, Gellert E, Burchill P, Challis K, Review of advanced composite structures for naval ships and submarines, Comp. Struct., 2001, 21-41
.3. Graham-Jones J, Summerscales J, Marine Applications of Advanced Fibre-Reinforced Composites, Woodhead Publishing, 2016, ISBN 9781782422501, https://doi.org/10.1016/B978-1-78242-250-1.09988-9
4. Pemberton R, Summerscales J, Graham-Jones J, Marine Composites, Woodhead Publishing, 2019, ISBN 9780081022641, https://doi.org/10.1016/B978-0-08-102264-1.09991-
5. Davies P, Rajapakse YDS, Editors, Durability of composites in a marine environment, 2014, Springer Dordrecht.
6. Davies P, Rajapakse YDS, Editors, Durability of composites in a marine environment 2, 2018, Springer Dordrecht.
7. Weitsman Y., Editor, Fluid Effects in Polymers and Polymeric Composites, Springer, 2012.
8. Colin X, Verdu J, Humid ageing of organic matrix composites, Chapter 3 in ref. [5], 2014, pp47-114.
9. Cocaud J, Célino A, Fréour S, Jacquemin F. What about the relevance of the diffusion parameters identified in the case of incomplete Fickian and non-Fickian kinetics? Journal of Composite Materials. 2019;53(11):1555-1565. doi:10.1177/0021998318805823.
10. Chen C, Springer G, Moisture and desorption of composite materials. J. Comp Mats. 1976;10:2-20.
11. Dona K, Du E, Carlsson LA, Fletcher DM, Boardman RP, Modeling of water wicking along fiber/matrix interface voids in unidirectional carbon/vinyl ester composites. Microfluidics and Nanofluidics. 2020;24(5):1-9.

12. Gellert EP, Turley DM. Seawater immersion ageing of glass-fibre reinforced polymer laminates for marine applications. Composites 1999;30A:1259.
13. Davies P, Mazeas F, Casari P, Sea Water Aging of Glass Reinforced Composites: Shear Behaviour and Damage Modelling. Journal of Composite Materials. 2001;35(15):1343-1372. doi:10.1106/MNBC-81UB-NF5H-P3ML
14. Kootsookos, Mouritz A, Seawater durability of glass and carbon polymer composites. Comp Sci & Tech. 2004;64:1503–1511.
15. Azevedo CB, Almeida Jr JHS, Flores HF, Eggers F, Amico SC. Influence of mosaic pattern on hygrothermally-aged filament wound composite cylinders under axial compression. Journal of Composite Materials. 2020;54(19):2651–2659. https://doi.org/10.1177/0021998319899144
16. Fahmi AA, Hurt JC, Stress Dependence of Water Diffusion in Epoxy Resin. Polymer Composites. 1980;1:77-80.
17. Yaniv G, Ishai O. Coupling between stresses and moisture diffusion in polymeric adhesives. Polym Eng Sci. 1987;27(10):731–9.
18. Humeau C, Davies P, Jacquemin F. An experimental study of water diffusion in carbon/epoxy composites under static tensile stress. Compos Part A Appl Sci Manuf. 2018 Apr 1;107:94–104. Available from https://www.sciencedirect.com/science/article/pii/S1359835X17304517
19. Suri C, Perreux D. The effects of mechanical damage in a glass fibre/epoxy composite on the absorption rate. Compos Eng. 1995;5(4):415–24.
20. Scott DW, Lai JS, Zureick A-H. Creep Behavior of Fiber-Reinforced Polymeric Composites: A Review of the Technical Literature. Journal of Reinforced Plastics and Composites. 1995;14(6):588-617. doi:10.1177/073168449501400603
21. Tuttle, M.E., Brinson, H.F. Prediction of the long-term creep compliance of general composite laminates. Experimental Mechanics. 1986;26:89–102. Available from https://doi.org/10.1007/BF02319961
22. Dillard DA, Viscoelastic behaviour of laminated composite materials, Ch. 8 in Fatigue of Composite Materials, ed Reifsnider KL, Elsevier, 1991.
23. Schapery RA. On the characterization of nonlinear viscoelastic materials. Polym Eng Sci. 1969;9(4):295–310. Available from http://doi.wiley.com/10.1002/pen.760090410
24. Jurf RA, Vinson JR. Effect of moisture on the static and viscoelastic shear properties of epoxy adhesives. J Mater Sci. 1985;20(8).

25. Sun T, Yu C, Yang W, Zhong J, Xu Q. Experimental and numerical research on the nonlinear creep response of polymeric composites under humid environments. Compos Struct. 2020; 251. Available from https://doi.org/10.1016/j.compstruct.2020.112673

26. Kim H, Takemura K. Influence of water absorption on creep behaviour of carbon fiber/epoxy laminates. Procedia Eng. 2011;10:2731–6. http://dx.doi.org/10.1016/j.proeng.2011.04.455

27. Keller MW, Jellison BD, Ellison T. Moisture effects on the thermal and creep performance of carbon fiber/epoxy composites for structural pipeline repair. Compos Part B Eng 2013, 45(1):1173–80. Available from https://www.sciencedirect.com/science/article/pii/S1359836812005008

28. Eggers F, Almeida Jr JHS, Lisbôa TV, Amico SC. Creep and Residual Properties of Filament-Wound Composite Rings under Radial Compression in Harsh Environments. Polymers. 2021 ; 13(1):33. https://doi.org/10.3390/polym13010033.

29 Ornaghi HL, Almeida JHS, Monticeli, FM *et al.* Time-temperature behavior of carbon/epoxy laminates under creep loading. Mech Time-Depend Mater. 2021 ;25**:**601–615. https://doi.org/10.1007/s11043-020-09463-z.

30. Miyano Y, Nakada M, Durability of Fiber-Reinforced Polymers, Wiley-VCH, Weinheim, Germany, 2018.

31. Woo EM. Moisture-temperature equivalency in creep analysis of a heterogeneous-matrix carbon fibre/epoxy composite. Composites. 1994;25(6):425–30.

32. Raghavan J, Meshii M. Time-dependent damage in carbon fibre-reinforced polymer composites. Compos Part A Appl Sci Manuf. 1996;27(12):1223–7.

33. Asadi A, Raghavan J. Influence of time-dependent damage on creep of multidirectional polymer composite laminates. Compos Part B Eng. 2011;42(3):489–98.

34. Zaoutsos S. Effect of multiple step creep/creep recovery loading on non-linear viscoelastic response of carbon fibre reinforced polymers. Plast Rubber Compos. 2013 Oct;42(8):315–22.

35. Tanks J, Rader K, Sharp S, Sakai T. Accelerated creep and creep-rupture testing of transverse unidirectional carbon/epoxy lamina based on the stepped isostress method. Compos Struct. 2017 Jan 1; 159:455–62. Available from https://www.sciencedirect.com/science/article/pii/S0263822316303166

36. Guedes RM Lifetime predictions of polymer matrix composites under constant or monotonic load. Composites: Part A 2006; 37:703-715.

37. Spoljaric S, Genovese A, Shanks RA. Polypropylene-microcrystalline cellulose composites with enhanced compatibility and properties. Compos. A Appl. Sci. Manuf. 2009; 40:791–799.

38. Wong S, Shanks R. Creep behaviour of biopolymers and modified flax fibre composites. Compos.

Interfaces. 2008; 15:131–145.

39. Findley W, Lai J, Onaran K, Christensen R. Creep and relaxation of nonlinear viscoelastic materials with an introduction to linear viscoelasticity. Journal of Applied Mechanics. 1977; 44(2).

40. Ornaghi HL, Almeida JHS, Monticeli, FM *et al.* Time-temperature behavior of carbon/epoxy laminates under creep loading. Mech Time-Depend Mater. 2021 ;25**:**601–615. https://doi.org/10.1007/s11043-020-09463-z.

41. Ornaghi Jr HL, Almeida Jr H, Monticeli FM, Neves RM. Stress relaxation, creep, and recovery of carbon fiber non-crimp fabric composites. Composites Part C: Open Access. 2020 Nov 1;3. 100051. https://doi.org/10.1016/j.jcomc.2020.100051.

42. Almeida Jr JH, Ornaghi HL, Lorandi N, Marinucci G and Amico S. On creep, recovery, and stress relaxation of carbon fiber-reinforced epoxy filament wound composites. Polym Eng Sci. 2018;58: 1837-1842. https://doi.org/10.1002/pen.24790.

43. Ornaghi Jr HL, Neves RM, Monticeli FM, Almeida H. Viscoelastic characteristics of carbon fiber-reinforced epoxy filament wound laminates. Composites Communications. 2020;21:1-8. https://doi.org/10.1016/j.coco.2020.100418.

44. Lagarias JC, Reeds JA, Wright MH, Wright PE. Convergence properties of the nelder-mead simplex method in low dimensions. SIAM Journal of Optimization. 1998; 9 :112–147.